BMB
Reports

BMB Rep. 2022; 55(10): 500-505
www.bmbreports.org

UCP2 KO mice exhibit ameliorated obesity and inflammation induced by high-fat diet feeding

Do Hyun Kim[1,2,3], *Hye Jin Kim*[2,3] *& Je Kyung Seong*[1,2,3,4,*]

[1]The Research Institute for Veterinary Science, College of Veterinary Medicine, Seoul National University, Seoul 08826, [2]Laboratory of Developmental Biology and Genomics, BK21 Program for Veterinary Science, College of Veterinary Medicine, Seoul National University, Seoul 08826, [3]Korea Mouse Phenotyping Center (KMPC), Seoul National University, Seoul 08826, [4]Interdisciplinary Program for Bioinformatics, Program for Cancer Biology, BIO-MAX/N-Bio Institute, Seoul National University, Seoul 08826, Korea

Uncoupling protein 2 (Ucp2) was first introduced as a member of Uncoupling protein family and a regulator of ROS formation; however, its role in adipose tissue is not fully understood. In the present study, we have investigated the role of Ucp2 against high-fat diet (HFD)-induced obesity in epididymal white adipose tissue (eWAT) and browning of inguinal white adipose tissue (iWAT). Diet-induced obesity is closely related to macrophage infiltration and the secretion of pro-inflammatory cytokines. Macrophages surround adipocytes and form a crown-like-structure (CLS). Some reports have suggested that CLS formation requires adipocyte apoptosis. After 12 weeks of HFD challenge, Ucp2 knockout (KO) mice maintained relatively lean phenotypes compared to wild-type (WT) mice. In eWAT, macrophage infiltration, CLS formation, and inflammatory cytokines were reduced in HFD KO mice compared to HFD WT mice. Surprisingly, we found that apoptotic signals were also reduced in the Ucp2 KO mice. Our study suggests that Ucp2 deficiency may prevent diet-induced obesity by regulating adipocyte apoptosis. However, Ucp2 deficiency did not affect the browning capacity of iWAT. [BMB Reports 2022; 55(10): 500-505]

INTRODUCTION

Uncoupling protein 2 (Ucp2) is encoded by a mitochondrial gene and was first reported as a regulator of mitochondrial proton leakage, ATP production, and insulin secretion (1). Although the exact mechanisms underlying these functions have not yet been understood, many researchers have agreed that *Ucp2* expression is negatively correlated with ROS and NO production (2, 3). In addition, the lifespan of Uncoupling protein 2 (Ucp2) knock-out (KO) mice is shorter than that of wild-type (WT) mice (4). However, Ucp2 displays a wide tissue expression range (5), and its roles in various tissues and cell types have not been covered.

Adipose tissue is a major metabolic organ that stores energy in the form of triglycerides (6-8). Its function in energy homeostasis of the whole body has been studied for decades and it is now considered an endocrine organ that secretes various adipokines and lipid metabolites (9, 10). Another key aspect of adipose tissue is the thermogenic capacity (11-13) of brown adipose tissue (BAT), which means dissipation of excess energy in the form of heat. The activation of BAT and recruitment of beige adipocytes from white adipocytes occur in an uncoupling protein 1 (Ucp1)-dependent manner (14-16). Recently, a study has revealed that macrophage-specific deletion of Ucp2 does not affect adipose tissue inflammation or weight gain after a high-fat diet (HFD) (17). To study the role of Ucp2 in adipose tissue, we have examined HFD-induced obesity and β3 adrenergic stimulation in Ucp2 KO mice. We have demonstrated that Ucp2 deletion dysregulates adipose tissue homeostasis under diet-induced obesity (DIO), but does not affect the browning of white adipose tissue (WAT).

Our study also showed that Ucp2 deletion alleviates HFD-induced weight gain and adipose tissue inflammation by blocking adipocyte apoptosis, an event preceding the recruitment of macrophages and proinflammatory cytokine secretion. We also establish the role of Ucp2 in thermogenesis and browning of inguinal white adipose tissue (iWAT), a well-known function of Ucp1, from the same family. Under β3-specific stimulation or 4°C cold exposure, browning capacity of iWAT of Ucp2 deficient mice was comparable to that of WT mice.

RESULTS

UCP2 KO mice were protected from HFD-induced obesity

To investigate the role of Ucp2 in adipose tissue under HFD condition, 6-week-old C57BL/7 mice were fed either normal chow diet (NCD) or high-fat diet for 16 weeks. We then isolated adipocytes and stromal vascular fraction (SVF) from epididymal white adipose tissue (eWAT) and measured *Ucp2* mRNA levels

*Corresponding author. Tel: +82-2-885-8395; Fax: +82-2-885-8397; E-mail: snumouse@snu.ac.kr

https://doi.org/10.5483/BMBRep.2022.55.10.056

Received 23 March 2022, Revised 19 April 2022, Accepted 7 June 2022

Keywords: Adipose, High fat diet, Inflammation, Mouse, Obesity, UCP2

ISSN: 1976-670X (electronic edition)

(Fig. 1A). Ucp2 expression was higher in HFD adipocytes. To confirm Ucp2 expression in adipocytes, we used a 3T3L1 cell line and verified a positive correlation between mRNA levels of *Ucp2* and *Pparγ*, a differentiation marker (Fig. 1B, C). Then, we randomly assigned 6-week-old WT and KO mice to either NCD or HFD for 12 weeks. A chronic access to HFD resulted in significant weight gain in WT mice compared to mice with NCD, whereas the weight gain in HFD KO mice was comparable to that in NCD group (Fig. 1D, E). The net body weight change by the NCD or HFD administration was also significantly less in the KO group (Fig. 1F). Body composition data also coincided with the changes in body weight. Ucp2 KO mice showed significantly lower fat mass and higher lean mass than WT mice (Fig. 1G). WAT in KO mice was lesser than it was in WT mice (Fig. 1H). The WAT weight of HFD KO mice was significantly lower than that of HFD WT mice (Fig. 1I). Serum triglyceride (TG) and glucose levels were also lower in HFD KO mice than in HFD WT mice (Supplementary Fig. 1G, H). The mRNA level of the eWAT glucose uptake marker, Glut4, was increased in HFD KO mice compared to that in NCD KO mice, but the expression level in HFD KO mice was also significantly lower than that in HFD WT mice (Supplementary Fig. 2D). Hematoxylin and eosin (H&E) staining also revealed that adipocytes were smaller in HFD KO mice (Fig. 1J, K).

HFD-induced macrophage infiltration and inflammation were reduced in HFD KO mice

As HFD-induced obesity is closely linked to macrophage infiltration and secretion of pro-inflammatory cytokines (18, 19), we analyzed the macrophages present in epididymal adipose tissue. Localization of antigen F4/80 using immunohistochemistry (IHC) staining showed crown-like-structure (CLS) formation in macrophages (Fig. 2A), and the number of CLSs was comparable in NCD WT and KO mice, while HFD KO mice showed a significant reduction in CLS formation compared to HFD WT (Fig. 2B). The mRNA level of *CCL2*, a marker for macrophage recruitment to adipose tissue, was significantly reduced in HFD KO mice compared to that in HFD WT mice (Fig. 2E). Additionally, mRNA levels of pro-inflammatory markers, TNFα, IFNγ, and IL-1β were also significantly decreased in KO mice (Fig. 2C), and mRNA level of the anti-inflammatory marker adiponectin in both HFD groups was similarly reduced, compared to that in NCD groups (Fig. 2D). Many studies have shown that in DIO, adipocyte apoptosis is a major cause of and a direct upstream step before CLS formation (20-22). To determine whether deletion of the *Ucp2* gene affects CLS formation and secretion of cytokines directly, or an upstream event, we investigated mRNA and protein levels of apoptotic signals in adipose tissue. We observed that caspase 3 (Cas3), caspase 9 (Cas9), and Bax/BCL2, the major apoptosis markers, only increased in the HFD WT group (Fig. 2F). TUNEL assay was also performed, and apoptotic expression was higher in HFD WT mice compared to that in KO mice.

Under β3 adrenergic receptor stimulation, Ucp2 does not affect the thermogenic capacity

To stimulate the β3 adrenergic receptor, we injected CL 316,243, a β3 adrenergic agonist, intraperitoneally (i.p.) into 7-week-old mice, once a day (1 mg/kg) for three consecutive days. A schematic is shown in Fig. 3A. Body weight gains or losses were measured before the first injection and at the time of euthanasia. Saline-injected WT and KO mice gained comparable weights, whereas CL-injected KO mice lost significantly more weight than CL-injected WT mice did (Fig. 3B). The body compositions were also measured; fat content of CL-injected KO mice tended

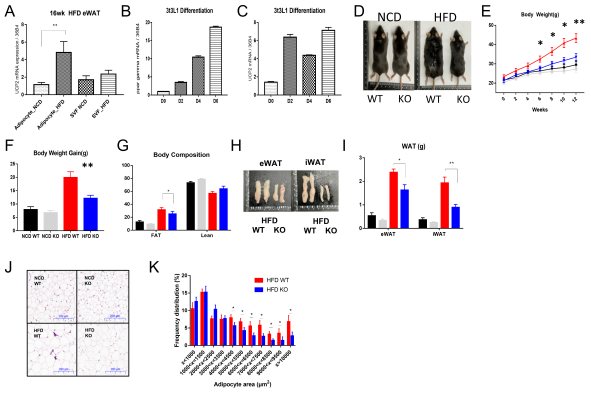

Fig. 1. UCP2 KO mice were protected from high fat diet (HFD)-induced obesity. (A) 6-week-old C57BL6 mice were fed an HFD for 16 weeks, adipocytes and SVF from eWAT were isolated, and Ucp2 mRNA expression was analyzed (n = 5 for NCD and n = 11 for HFD). 3T3L1 cells were differentiated and the mRNA expression levels of the (B) differentiation marker Pparγ and (C) Ucp2 were detected. (D) Photographs of WT and KO mice after 2 weeks of NCD and HFD. (E) Body weight graph of 6-18-week-old mice in each group. (F) Graph of body weight gain throughout the experiment. (G) Body composition data. (H) Photographs of WAT of HFD-induced WT and KO mice. (I) WAT weight graph. (J) H&E staining of epididymal adipose tissue. (K) Adipocyte sizes were quantified. Data are presented as the mean ± SEM. *P < 0.05, **P < 0.01, ***P < 0.001.

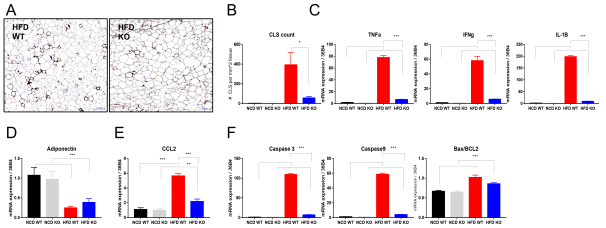

Fig. 2. An epididymal adipose tissue macrophage is reduced in HFD treated KO mice. (A) F4/80 IHC staining of crown-like structure (CLS) formation in eWAT. (B) Number of CLSs was analyzed. (C) Relative mRNA expression of pro-inflammatory markers (M1 polarization). (D) Relative mRNA expression of anti-inflammatory markers (M2 polarization). (E) CCl2 mRNA expression. (F) Relative mRNA expression of apoptosis markers. Data are presented as the mean ± SEM. *P < 0.05, **P < 0.01, ***P < 0.001.

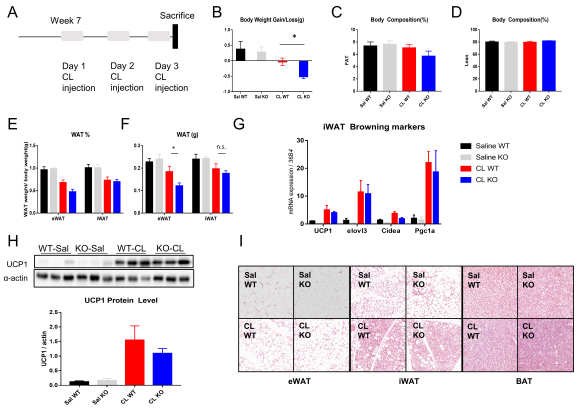

Fig. 3. No difference was observed in CL 316,243-induced β3 adrenergic stimulation between the two genotypes. (A) Schematic diagram of CL injection experiment. (B) Body weight gain graph, (C) fat composition, (D) lean composition. (E) WAT weight differences normalized by total body weight, and (F) absolute fat weight differences of Saline injected WT, Saline injected KO, CL injected WT, and CL injected KO mice. (G) Relative mRNA expression of browning markers and (H) UCP1 protein expression in iWAT was normalized to the levels of α-actin. (I) H&E staining of eWAT, iWAT, and BAT. Data are presented as the mean ± SEM. *P < 0.05, **P < 0.01, ***P < 0.001.

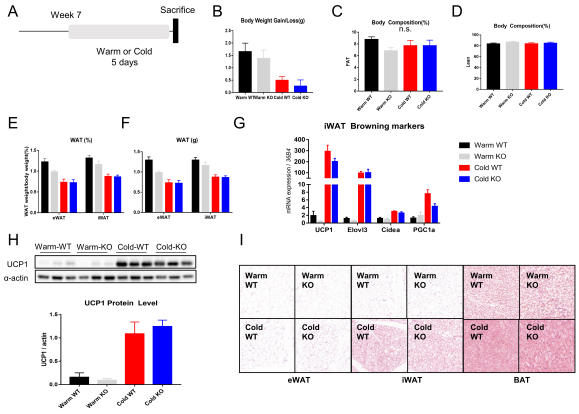

Fig. 4. Cold-induced browning capacity was comparable between WT and KO mice. (A) Schematic diagram of cold-induced browning. (B) Body weight gain graph. Body composition of (C) fat, (D) lean, (E) weights of WAT normalized by body weight and (F) actual weights are listed. (G) Relative mRNA expression of browning markers was analyzed in iWAT. (H) UCP1 protein expression in iWAT was normalized to the levels of α-actin. (I) H&E staining of eWAT, iWAT, and BAT. Data are presented as the mean ± SEM.

to be lower than that of CL-injected WT mice, but these differences were not statistically significant (Fig. 3C), while lean masses were similar among all groups (Fig. 3D). Their actual WAT masses were measured and normalized by their body weights and actual weights were recorded (Fig. 3E, F). We then measured browning of inguinal iWAT at the molecular level. Saline-injected WT and KO mice showed insignificant levels of Ucp1, whereas CL-injected WT and KO mice both showed high expression of Ucp1, at comparable levels (Fig. 3H). The mRNA levels of the browning markers, *Ucp1*, *Elovl3*, *CIDEA*, and *PGC1α*, were consistent with the corresponding protein levels (Fig. 3G). Finally, we histologically investigated the browning of adipose tissue and confirmed that adipocyte sizes and lipid droplet accumulations were similar between the two genotypes (Fig. 3I).

Ucp2 deletion does not affect phenotypes or browning of WAT under cold adaptation

To explore the role of Ucp2 in cold adaptation, we exposed 7-week-old mice to warm (30°C) and cold (4°C) conditions for 5 days. A schematic is shown in Fig. 4A. This cold exposure did not affect body weight changes in WT and KO mice (Fig. 4B). Changes in body composition data and actual WAT weight were negligible (Fig. 4C-F). Protein and mRNA levels of browning markers showed similar cold effects in both the WT and KO groups and showed no differences between the two genotypes (Fig. 4G, H). Finally, we compared histological differences, however; we found no evidence that Ucp2 deletion affects adipose tissue remodeling (Fig. 4I).

DISCUSSION

In the past decades, studies have revealed the significance of genes from *Ucp* family. *Ucp1* is specifically expressed in brown and beige adipocytes, *Ucp3* expression is distributed in skeletal muscles, and *Ucp2* expression has a wide tissue distribution (5). Many studies have studied the roles of Ucp2 in various organs (23-25) and they have demonstrated that Ucp2 negatively regulates ROS formation (2-4). However, the role of Ucp2 in adipose tissue and energy metabolism was not fully investigated.

In 2001, a cross between Ucp2 KO and ob/ob mice was studied, which showed a gain of weight comparable to that of WT mice (1). In 2002, Ucp2 KO mice were reported to have higher body weights than WT mice after the HFD challenge (26). These results contradict our observation that Ucp2 KO mice gained significantly less weight than Ucp2 WT mice did after the HFD challenge. These discrepancies may be attributed to two reasons. Firstly, the Ucp2 KO mice used in each experiment had different backgrounds. In 2009, Pi *et al*. discovered that the insulin secretion capacities of Ucp2 KO mice differed according to their genetic backgrounds (27). Among 129/B6 mixed, 129 congenic, B6 congenic, and A/J congenic Ucp2 KO mice, only 129/B6 mixed genetic background, the one used in the two previously reported articles, showed a higher insulin secretion compared to WT mice. Secondly, all three studied used different experimental designs. The first group used ob/ob mice with NCD, and the second group fed HFD to 4-month-old mice for 4.5 months. We fed HFD to 6-week-old mice for 2 months. We suggest that these two differences may have resulted in the inconsistent results of the studies.

Adipose tissue is a metabolically active and dynamic organ

that comprises heterogeneous cell population (28). Adipocytes, making up the majority of cell populations, store energy in the form of triglycerides (7), whereas the rest of the populations are composed of various cell types, including immune cells (9, 28-30). Recently, a study has reported that macrophage-specific *Ucp2* deletion does not affect body weight gain and adipose tissue inflammation after HFD (17), whereas our data demonstrated that *Ucp2* null KO mice were protected from DIO. To delineate this matter, we fed 6-week-old C57/BL6 mice HFD for short (2 weeks) and long (16 weeks) terms and isolated them into adipocytes and a SVF from eWAT. Although the *Ucp2* mRNA levels in adipocytes and SVF of the NCD group were comparable, after the HFD challenge, adipocytes exhibited significantly higher *Ucp2* levels than the SVF (Fig. 1A, Supplementary Fig. 1E). In addition, we used 3T3-L1 murine pre-adipocytes and confirmed that *Ucp2* mRNA expression was increased by the *PGC1α* mRNA level, a marker for differentiation (Fig. 1B, C). Considering the expression levels of Ucp2 in adipocytes, it may play a role in adipocytes but not in SVF, including macrophages, in HFD-induced obesity.

We induced obesity in Ucp2 WT and KO mice through HFD. Surprisingly, HFD treated KO mice exhibited leaner phenotypes compared to WT mice. Weight gain was significantly reduced in Ucp2 KO mice compared to that in WT mice (Fig. 1D-F). Serum TG and glucose levels were significantly lower in the HFD KO group (Supplementary Fig. 1G, H), and the eWAT glucose uptake marker level was also reduced in HFD KO mice (Supplementary Fig. 2D). HFD KO mice had significantly lower fat content (Fig. 1G) and WAT weights (Fig. 1I). Histologically, HFD KO mice showed smaller adipocyte distribution (Fig. 1J, K).

Obesity is strongly associated with pro-inflammatory cytokines and adipose tissue macrophages (18, 31). Moreover, deletion of macrophages has been reported to prevent DIO phenotypes in eWAT (32). It has also been reported that adipocyte apoptosis is an upstream event necessary for macrophage infiltration into adipose tissue and CLS formation (20-22). Furthermore, Ucp2 was reported to regulate adipocyte apoptosis in 3T3L1 cell lines when treated with 1alpha,25-dihydroxyvitamin D3 (33). We confirmed that adipose tissue macrophages (Fig. 2A, B) and pro-inflammatory markers (Fig. 2C) were reduced in HFD KO mice than in HFD WT mice. We then compared apoptosis between the two genotypes. Interestingly, HFD KO mice showed significantly reduced mRNA and protein expression of apoptosis markers compared to HFD WT mice (Fig. 2F, Supplementary Fig. 2A, B). TUNEL assay also showed higher apoptotic signals in the HFD WT group (Supplementary Fig. 2C).

Sympathetic nervous system stimulation via β-adrenergic receptors induces multilocular lipid droplets in adipocytes and browning of white adipose tissue. Ucp1, a well-known marker for browning of WAT, dissipates heat by uncoupling the H+ gradient, which would otherwise be used in ATP synthesis. Recently, Caron S *et al*. reported that Ucp2 KO mice failed to adapt to chronic cold exposure (10°C) (34). This study focused on glucose metabolism in BAT and did not reveal the role of Ucp2 in iWAT and thermogenesis. Here, using stimulation with a β3 adrenergic agonist and 4°C cold exposure, we demonstrated that the browning capacity of iWAT is comparable between WT and KO mice. Ucp2-depleted mice showed a tendency to lose more weight than WT mice (Fig. 3B and 4B), but the actual weights of WAT and adipocyte sizes were comparable (Fig. 3F, I; 4F, I). Moreover, the protein and mRNA expression of major browning markers in iWAT were comparably increased (Fig. 3G, H; 4G, H).

In conclusion, Ucp2 deficiency ameliorated HFD-induced obesity in eWAT but did not alter thermogenic and browning capacities in iWAT. HFD-challenged Ucp2 KO mice showed lean phenotypes in terms of body weight, fat composition, actual fat weight, and smaller adipocytes. Additionally, macrophage infiltration, CLS formation, pro-inflammatory cytokine markers, and apoptosis markers were reduced in the eWAT of the HFD-KO mice. Considering the high expression levels of Ucp2 in HFD adipocytes, we suggest that Ucp2 may regulate apoptotic pathways of adipocytes and eventually prevent HFD-induced obesity.

MATERIALS AND METHODS

Animals

Ucp2 null KO mice were purchased from the Jackson Laboratory, USA (B6.129S4-Ucp2tm1Lowl/J, Strain #:005934). Ucp2 KO mice were obtained by crossing heterozygous breeders. All protocols were performed in accordance with the Guide for Animal Experiments (edited by the Korean Academy of Medical Sciences and approved by the Institutional Animal Care and Use Committee of Seoul National University, Seoul, Korea) (approval number: SNU-201013-2-1). For HFD experiments, 6-week-old male WT and KO mice were randomly assigned (n = 5) to either NCD or a 60% HFD (20% carbohydrate, 60% fat, 20% protein; D12492; Research Diets Inc.). For CL 316,243 (Sigma, USA) treatment, 7-week-old WT and KO mice were i.p. injected with 1 mg/kg of CL for 3 days (n = 4). For the cold challenge, 7-week-old WT and KO mice were randomly assigned to either thermoneutral (30°C) or cold (4°C) environment conditions for 5 consecutive days (n = 5). At the end of each experiment, the body composition of all animals was determined by nuclear magnetic resonance (Minispec LF-50, Bruke).

Histology

Samples were fixed with 4% paraformaldehyde and embedded in paraffin. They were sliced into 4.5-μm-thin sections and stained with H&E, following a standard protocol. For IHC staining, anti-F4/80 antibody (D2S9R, Cell Signaling Technology) was used. The samples were then washed and blocked with 2.5% horse serum for 1 h. After another washing with PBS + 0.05% Tween 20 incubation was performed with a 1:500 dilution of primary anti-F4/80 overnight in a 4°C chamber. Samples were washed and incubated with secondary antibody (ImmPRESS,

Vector Laboratories) for 1 h at 24°C. Finally, they were developed using a DAB kit (Vector Laboratories), according to the manufacturer's protocols. H&E and IHC samples were visualized using a Pannoramic Scanner (3DHISTECH).

Western blotting

Proteins were extracted using RIPA buffer and quantified using the BCA assay protocol. Equal amounts of protein were separated by SDS-PAGE and then transferred to PVDF membranes. Samples were incubated with primary antibodies overnight at 4°C and then incubated with HRP-conjugated secondary antibodies. The blots were visualized using enhanced chemiluminescence and a Chemi-Doc Imaging System (Bio-Rad). Images were quantified and normalized using the ImageJ software (NIH). The primary antibodies used were UCP1 (Abcam), Caspase3 (Cell Signaling Technology), Cleaved caspase 3 (CST), α-actin (Sigma), and β-tubulin (Abbkine).

Quantitative real-time PCR

Total RNA was extracted from the tissues using TRIzol reagent (Invitrogen) according to the manufacturer's instructions. cDNA was synthesized using a premix (Bioneer), according to the manufacturer's protocol. qPCR was performed using the QuantStudio5 (Applied Biosystems). PCR was performed using the SYBR Lo-ROX Kit (Meridian), according to the manufacturer's instructions. The primer sequences used are shown in the Supplementary Fig. 3.

ACKNOWLEDGEMENTS

This study was partially supported by the Research Institute for Veterinary Science, Seoul National University. This study was supported by the Korea Mouse Phenotyping Project (NRF-2013 M3A9D5072550) of the Ministry of Science and ICT, through the National Research Foundation.

CONFLICTS OF INTEREST

The authors have no conflicting interests.

REFERENCES

1. Zhang CY, Baffy G, Perret P et al (2001) Uncoupling protein-2 negatively regulates insulin secretion and is a major link between obesity, beta cell dysfunction, and type 2 diabetes. Cell 105, 745-755
2. Bai Y, Onuma H, Bai X et al (2005) Persistent nuclear factor-kappa B activation in Ucp2-/- mice leads to enhanced nitric oxide and inflammatory cytokine production. J Biol Chem 280, 19062-19069
3. Arsenijevic D, Onuma H, Pecqueur C et al (2000) Disruption of the uncoupling protein-2 gene in mice reveals a role in immunity and reactive oxygen species production. Nat Genet 26, 435-439
4. Andrews ZB and Horvath TL (2009) Uncoupling protein-2 regulates lifespan in mice. Am J Physiol Endocrinol Metab 296, E621-E627
5. Erlanson-Albertsson C (2002) Uncoupling proteins–a new family of proteins with unknown function. Nutr Neurosci 5, 1-11
6. Choe SS, Huh JY, Hwang IJ, Kim JI and Kim JB (2016) Adipose tissue remodeling: its role in energy metabolism and metabolic disorders. Front Endocrinol (Lausanne) 7, 30
7. Cohen P and Spiegelman BM (2016) Cell biology of fat storage. Mol Biol Cell 27, 2523-2527
8. Cha JH, Jeong Y, Oh AR, Lee SB, Hong SS and Kim K (2021) Emerging roles of PHLPP phosphatases in metabolism. BMB Rep 54, 451-457
9. Prunet-Marcassus B, Cousin B, Caton D, Andre M, Penicaud L and Casteilla L (2006) From heterogeneity to plasticity in adipose tissues: site-specific differences. Exp Cell Res 312, 727-736
10. Lee MJ, Wu Y and Fried SK (2013) Adipose tissue heterogeneity: implication of depot differences in adipose tissue for obesity complications. Mol Aspects Med 34, 1-11
11. Himms-Hagen J (1985) Brown adipose tissue metabolism and thermogenesis. Annu Rev Nutr 5, 69-94
12. Bartelt A and Heeren J (2014) Adipose tissue browning and metabolic health. Nat Rev Endocrinol 10, 24-36
13. Hossain M, Imran KM, Rahman MS, Yoon D, Marimuthu V and Kim YS (2020) Sinapic acid induces the expression of thermogenic signature genes and lipolysis through activation of PKA/CREB signaling in brown adipocytes. BMB Rep 53, 142-147
14. Fedorenko A, Lishko PV and Kirichok Y (2012) Mechanism of fatty-acid-dependent UCP1 uncoupling in brown fat mitochondria. Cell 151, 400-413
15. Madsen L, Pedersen LM, Lillefosse HH et al (2010) UCP1 induction during recruitment of brown adipocytes in white adipose tissue is dependent on cyclooxygenase activity. PLoS One 5, e11391
16. Chang SH, Jang J, Oh S et al (2021) Nrf2 induces Ucp1 expression in adipocytes in response to β3-AR stimulation and enhances oxygen consumption in high-fat diet-fed obese mice. BMB Rep 54, 419-424
17. van Dierendonck X, Sancerni T, Alves-Guerra MC and Stienstra R (2020) The role of uncoupling protein 2 in macrophages and its impact on obesity-induced adipose tissue inflammation and insulin resistance. J Biol Chem 295, 17535-17548
18. Weisberg SP, McCann D, Desai M, Rosenbaum M, Leibel RL and Ferrante AW Jr (2003) Obesity is associated with macrophage accumulation in adipose tissue. J Clin Invest 112, 1796-1808
19. Trayhurn P (2007) Adipocyte biology. Obes Rev 8 Suppl 1, 41-44
20. Xiao Y, Yuan T, Yao W and Liao K (2010) 3T3-L1 adipocyte apoptosis induced by thiazolidinediones is peroxisome proliferator-activated receptor-gamma-dependent and mediated by the caspase-3-dependent apoptotic pathway. FEBS J 277, 687-696
21. Lindhorst A, Raulien N, Wieghofer P et al (2021) Adipocyte death triggers a pro-inflammatory response and induces metabolic activation of resident macrophages. Cell Death Dis 12, 579

22. Alkhouri N, Gornicka A, Berk MP et al (2010) Adipocyte apoptosis, a link between obesity, insulin resistance, and hepatic steatosis. J Biol Chem 285, 3428-3438
23. Kim JG, Sun BH, Dietrich MO et al (2015) AgRP neurons regulate bone mass. Cell Rep 13, 8-14
24. Madreiter-Sokolowski CT, Gyorffy B, Klec C et al (2017) UCP2 and PRMT1 are key prognostic markers for lung carcinoma patients. Oncotarget 8, 80278-80285
25. Qin N, Cai T, Ke Q et al (2019) UCP2-dependent improvement of mitochondrial dynamics protects against acute kidney injury. J Pathol 247, 392-405
26. Joseph JW, Koshkin V, Zhang CY et al (2002) Uncoupling protein 2 knockout mice have enhanced insulin secretory capacity after a high-fat diet. Diabetes 51, 3211-3219
27. Pi J, Bai Y, Daniel KW et al (2009) Persistent oxidative stress due to absence of uncoupling protein 2 associated with impaired pancreatic beta-cell function. Endocrinology 150, 3040-3048
28. Eto H, Suga H, Matsumoto D et al (2009) Characterization of structure and cellular components of aspirated and excised adipose tissue. Plast Reconstr Surg 124, 1087-1097
29. Bora P and Majumdar AS (2017) Adipose tissue-derived stromal vascular fraction in regenerative medicine: a brief review on biology and translation. Stem Cell Res Ther 8, 145
30. Rondini EA and Granneman JG (2020) Single cell approaches to address adipose tissue stromal cell heterogeneity. Biochem J 477, 583-600
31. Wang Y, Tang B, Long L et al (2021) Improvement of obesity-associated disorders by a small-molecule drug targeting mitochondria of adipose tissue macrophages. Nat Commun 12, 102
32. Bu L, Gao M, Qu S and Liu D (2013) Intraperitoneal injection of clodronate liposomes eliminates visceral adipose macrophages and blocks high-fat diet-induced weight gain and development of insulin resistance. AAPS J 15, 1001-1011
33. Sun X and Zemel MB (2004) Role of uncoupling protein 2 (UCP2) expression and 1alpha, 25-dihydroxyvitamin D3 in modulating adipocyte apoptosis. FASEB J 18, 1430-1432
34. Caron A, Labbe SM, Carter S et al (2017) Loss of UCP2 impairs cold-induced non-shivering thermogenesis by promoting a shift toward glucose utilization in brown adipose tissue. Biochimie 134, 118-126